CYCLIC TESTING OF EXISTING AND RETROFITTED RIVETED STIFFENED SEAT ANGLE CONNECTIONS

By Majid Sarraf,[1] Associate Member, ASCE, and Michel Bruneau,[2] Member, ASCE

ABSTRACT: A typical riveted stiffened seat angle connection taken from an 83-year-old building was tested to investigate its actual hysteretic behavior and potential moment resistance. Results show that such existing connections can develop a considerable moment resistance, but pinched hysteretic curves indicate they have a relatively low energy dissipation capability. Analytical models for prediction of the moment capacity of these connections are also developed and predicted results based on these models are found to be in good agreement with the test results. Then, two retrofitting schemes are proposed to improve the connection's hysteretic behavior, and the adequacy of the suggested retrofits is verified experimentally. First, the addition of ductile knee-braces is investigated. A "selective welding" approach is developed as a second retrofitting technique. The design philosophy of each retrofitting scheme is explained, and analytical procedures to predict the moment capacity of retrofitted connections are presented. Experimentally obtained hysteretic curves are presented, improvements in the behavior of connections are noted, and comparison with analytical predictions are made.

INTRODUCTION

Riveted stiffened seat angle connections, commonly used as rigid connections in old steel frames, have been categorized as flexible connections by practicing engineers for many decades now. Although such connections are no longer desirable in today's moment-resisting steel-frame connections in seismic regions, there exist many old buildings originally built using this type of connections, whose seismic survival is essential. Engineers, when required to assess the seismic resistance of such buildings would typically ignore the lateral resistance of frames with this type of connection, which translates into a greater perception of seismic vulnerability, and could eventually lead to the demolition or need to perform major seismic retrofit for many steel buildings.

As these riveted stiffened seat angle connections, when present, are usually found at every beam-to-column joint throughout an entire building, it is conceivable that buildings constructed of steel frames having these connections could have adequate resistance and ductility to survive small to moderate earthquakes. However, analytical studies on the performance of steel frames having such connections and subjected to earthquakes cannot be conducted at this time, because the cyclic nonlinear inelastic moment-rotation relationship of such connections is unknown. Moreover, should these buildings be found to have a deficient seismic resistance in their as-is condition, ductile retrofit strategies specific to these connections, which could be implemented at a minimum disturbance to the occupants, are also lacking.

In that perspective, this paper first reports on the full-scale testing of existing riveted stiffened seat angle connections obtained from an existing building to establish the potential resistance of these connections and their typical hysteretic behavior. Then, with a view to applications in regions exposed to more severe seismic hazards, two ductile retrofitting techniques are proposed to enhance the hysteretic performance of these existing riveted stiffened seat angle connections: (1) The addition of ductile knee braces; and (2) a selective welding approach. These were obviously developed to correct the experimentally identified weaknesses of the existing connection while retaining its desirable features.

In this paper, the design philosophy for each proposed retrofit is outlined and the experimental results obtained from full-scale tests of connections taken from an existing building and retrofitted as proposed are presented. Also, analytical models of the observed behavior and ultimate moment resistance are proposed along with a newly developed physical model to predict the moment capacity of riveted stiffened seat angle connection to built-up column sections.

PRIOR STUDIES ON RIVETED AND SEMIRIGID CONNECTIONS

Only a few tests on riveted semirigid connections were found in the existing literature. Early investigations of these riveted connections to determine their rigidity started with a series of monotonic tests conducted by Moore and Wilson (1917) and later by Rathbun (1935) and Young and Jackson (1934). In that latter case, reverse loading was applied, to a limited level, on typical wind-resisting connections to assess their rigidity when subjected to wind loads.

Significantly more knowledge exists on the monotonic behavior of bolted semirigid connections, the first relevant tests apparently being conducted by Lewitt et al. (1966). Numerous tests have been conducted since then by other researchers [e.g., Marley and Gerstle (1982), Maxwell et al. (1981)] to enhance the understanding of the behavior of semirigid connections under monotonic loads. The results of these tests were then used by others to develop various experimentally based analytical models [e.g., cubic-B-spline model by Jones et al. (1982), and power model by Kishi and Chen (1990)]. However, all these existing experimentally based analytical models remain valid only for monotonically loaded connections, and their applicability to cyclically loaded connections is not established.

With the exception of the Young and Jackson (1934) test reported earlier, cyclic tests of semirigid connections are relatively recent. Radziminsky and Azizinamini (1986) conducted experiments on double angles with top and seat angle connections, and subjected this type of connection to low-amplitude cyclic rotations. Other researchers tested (Astaneh et al. 1989) and modeled (Stefano et al. 1994) double web angle connections under large inelastic cycles. Nader and Astaneh (1989) conducted shake-table experiments of frames with double web angle connections, as well as the same type of semirigid connections used by Radziminsky and Azizinamini (1986). Another study (Leon et al. 1994) investigates the in-

[1]Grad. Res. Asst., Ottawa Carleton Earthquake Engrg. Res. Ctr., Civ. Engrg. Dept., 161 Louis Pasteur, Univ. of Ottawa, Ottawa, Ontario K1N 6N5.
[2]Assoc. Prof., Ottawa Carleton Earthquake Engrg. Res. Ctr., Civ. Engrg. Dept., 161 Louis Pasteur, Univ. of Ottawa, Ottawa, Ontario K1N 6N5.

Note. Associate Editor: Amde M. Amde. Discussion open until December 1, 1996. To extend the closing date one month, a written request must be filed with the ASCE Manager of Journals. The manuscript for this paper was submitted for review and possible publication on August 22, 1994. This paper is part of the *Journal of Structural Engineering*, Vol. 122, No. 7, July, 1996. ©ASCE, ISSN 0733-9445/96/0007-0762–0775/$4.00 + $.50 per page. Paper No. 9068.

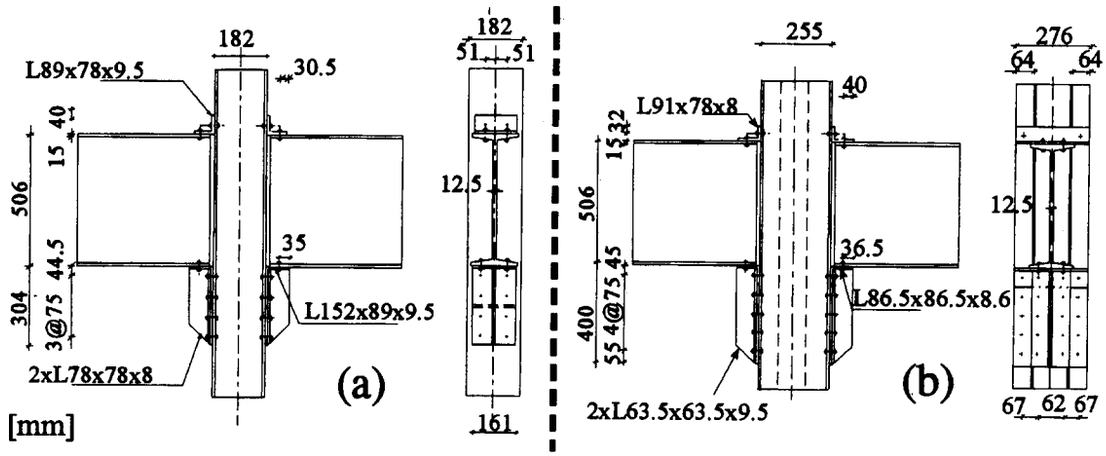

FIG. 1. Detail of Riveted Stiffened Seat Angle Connections: (a) Single Column Detail; (b) Built-Up Column Detail

elastic cyclic behavior of some selected types of bolted and riveted semirigid connections. Preliminary findings indicate that moment-rotation curves obtained for riveted connections are pinched due to slippage of the connection upon load reversal. This last experimental study is noteworthy since it is, with the work reported here, the only other known seismic-related hysteretic testing program of riveted connections. However, Leon et al. have simulated old connections by developing an in-laboratory capability for riveting new steel sections, and consequently cannot take into account any effect of aging of the rivets and base steel.

EXPERIMENTAL APPROACH

In this study the specimens were primarily part of a steel frame of the Daly Building, which was constructed in 1910 on the corner of Rideau and Sussex streets in downtown Ottawa and demolished in 1992. A limited number of specimens were obtained from that building, providing a unique opportunity for the experimental investigation reported here. Two specimens, in good condition, not rusted, and of slightly different joint configuration were obtained. Their details are included in Fig. 1. Obviously an extensive series of tests considering various parameters was not possible, but valuable information for seismic evaluation and retrofit purposes could be extracted from the specimens available.

PRELIMINARY TESTS

Two coupons of steel (one taken from the flange and one from the web of a typical beam) were machined to standard size tensile test specimen, in accordance with ASTM E8, and tested. The results indicated that the specimens are of a mild steel, with an average yield point, F_y, of 225 MPa and an average tensile strength, F_u, of 400 MPa. However, a normal plastic plateau was obtained, and elongation at failure was approximately 25%, putting to rest any suspicion that aging may have detrimentally affected the steel properties in this case. Also, another coupon of steel (taken from the flange) was prepared to test its weldability. It was machined into an ASTM E8 specimen, cut at the middle, and rejoined by performing a double-V joint configuration weld using E70 electrodes. Testing this specimen showed the weldability of the steel, as failure occurred in the base metal away from the weld. Although a standard ASTM procedure exists to test weldability, the foregoing was done for expediency. While this was sufficient for this experimental work, designers should be warned that a single coupon test does not provide the level of reliability needed in a design process.

To determine the tensile strength and stress of the rivets, a piece of steel plates connected by a single rivet was cut out from an existing connection. The selected rivet was tested in tension by pulling on the plates. Taking the 20 mm (3/4 in.) rivet hole area as the actual effective cross-section resisting area of rivet steel (instead of its nominal shank area), to account for the fact that the hot driven rivet may have filled its original 1.6 mm (1/16 in.) hole clearance (Kulak, et al. 1987), the yield and tensile strength of the rivet were calculated as 258 and 483 MPa, respectively. This indicates that the rivets present in the acquired specimens are comparable to ASTM A502 grade 1 rivets.

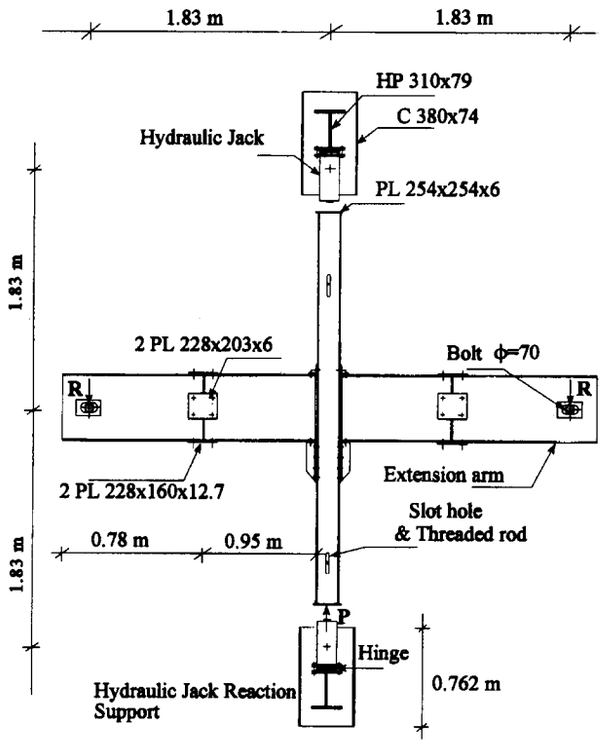

FIG. 2. Experiment Setup

TEST SETUP

The test setup used in this investigation (Fig. 2) mainly consists of two hinge supports, two single-way acting hydraulic jacks used to simplify detailing of the test setup and reaction supports, and the horizontally positioned specimen to be cyclically tested. In every cycle, each hydraulic jack is used to apply one-half of the load cycle by pushing at one end of

the column of the specimen, the other end being free, i.e., unrestrained from movement by the other jack. Reaction forces under this load develop at the hinge supports of the beams, which consist of large-diameter special bolts anchored to the laboratory strong floor. Consequently, the reaction forces applied at a certain distance from the column face, using the beams as lever arms, produce the moment of interest at the connections to be tested.

The hinge supports were detailed to allow some unrestrained movements in the direction of the beams' longitudinal axis, to avoid developing axial forces in the beams when the distance between the specimen and the hinge supports change slightly due to rigid-body rotations of the beams about their eccentric connection contact points during the test. Also, a number of rollers were placed between the specimen and the floor, to avoid developing friction forces during movement of the specimen.

The chosen test setup is not intended to simulate the effects of earthquakes on the columns of this subassembly, as the applied loading creates no shear or bending in the columns. However, the test setup definitely allows the simultaneous cyclic testing of two identical connections per specimen and investigation of their hystretic behavior in cases where the yielding of columns would not be an issue. The results in this paper must be interpreted in that context.

INSTRUMENTATION

A variety of instruments were installed to measure different parameters and facilitate monitoring and control of the test. Measurements were taken on load, rotations, displacements, and strains at points of interest. A total of 24 channels of data was recorded by a data-acquisition system. A detailed outline of all instruments is presented elsewhere (Sarraf 1993).

For all specimens, the moment-rotation (M-θ) relationship was chosen as a good descriptive and quantitative expression of the hystretic behavior and resistance for this type of connection. To establish the moment-rotation relationship for each connection in this experiment, the angle of rotation between the axes of a beam and the column is obtained from the relative displacements measured by a pair of linear voltage displacement transducers (LVDTs), installed just above and below the beam at the joint. Moments at the connections during the test were measured in two independent ways: (1) By multiplying hinge support reactions with their respective lever arm length to the column face; and (2) by converting into moments the strains measured by strain gauges near the connections on beam flanges.

The rotation values for the two connections simultaneously tested in each specimen were independently measured, but were always found to be nearly identical. Therefore, all M-θ relationships presented here are the average results obtained from the tested pairs of connections. For the following, an arbitrary sign convention is adopted for which positive moments produce tension in the top angles and compression in seat angles, and negative moments do the opposite.

EXPERIMENTAL RESULTS FOR EXISTING (NONRETROFITTED) CONNECTION

The experimentally obtained M-θ hysteretic curve for the existing connection is shown in Fig. 3(a). The loading history was designed and executed to create progressively larger yield excursions at each cycle, but the intensity of each excursion was adjusted during testing as interesting events or unsuspected behaviors were observed. Severe pinching of the hysteretic curves, even in the early stages of loading, is clearly observed.

Based on first observation of inelastic action, positive and negative yield rotations can be roughly defined as 6.15×10^{-3} and -6×10^{-3} rad, respectively. Tensile yielding of the rivets connecting the vertical leg of the top angles was detected by special custom-made clip gauges at $M^+ = 65$ kN·m. Similarly, tensile yielding of the first row of rivets under the seat angles was detected when $M^- = -95$ kN·m.

In positive flexure, the specimen was loaded until large deformations of the rivets in the top angles gave signs of impending tensile failure (Fig. 4). Loading was stopped at $M^+_{max} = 81.1$ kN·m, at a rotation of 21.28×10^{-3} rad. In negative flexure, the specimen was pushed to failure, which occurred due to shear failure of a rivet in the seat angle when the maximum negative moment (M^-_{max}) reached -139 kN·m, at a maximum negative rotation (θ^-_{max}) of -27.9×10^{-3} rad and a rotation ductility of 5. The evolution of this hysteretic behavior is explained in detail elsewhere (Sarraf 1993), but some important mechanisms of this behavior are described in the following section.

At this point, the specimen was repaired by simply replacing all rivets connecting the seat angle to the beam's bottom flange (a total of four rivets, including the failed rivet) with high-strength bolts. This was done to investigate the possible improvement in the negative moment capacity of the connection, and to find the next failure mode of this connection. Some positive moments were applied to the connections to see the effect of reversed cyclic loading on the seat connections, but since the specimen had highly deformed rivets and angles in the top part of the connections, the positive moment was kept below 47 kN·m to prevent their possible failure.

The M-θ curve based on the average rotation of the two connections for this case is shown in Fig. 3(b). The connections resisted a maximum moment (M^-_{max}) of -160 kN·m, corresponding to a rotation (θ^-_{max}) of -46×10^{-3} rad, and a rotation ductility of more than 7. At the peak of the negative excursion of the third cycle, the right-hand side connection

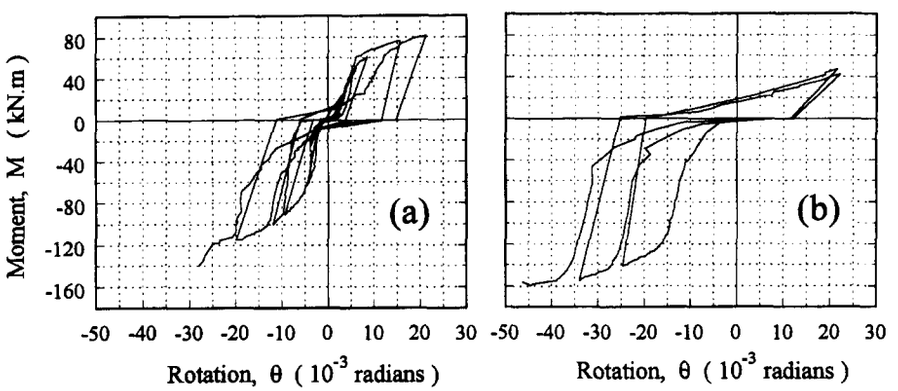

FIG. 3. Hysteretic Curves of Tested Connections: (a) Original Connections; (b) Repaired Connections

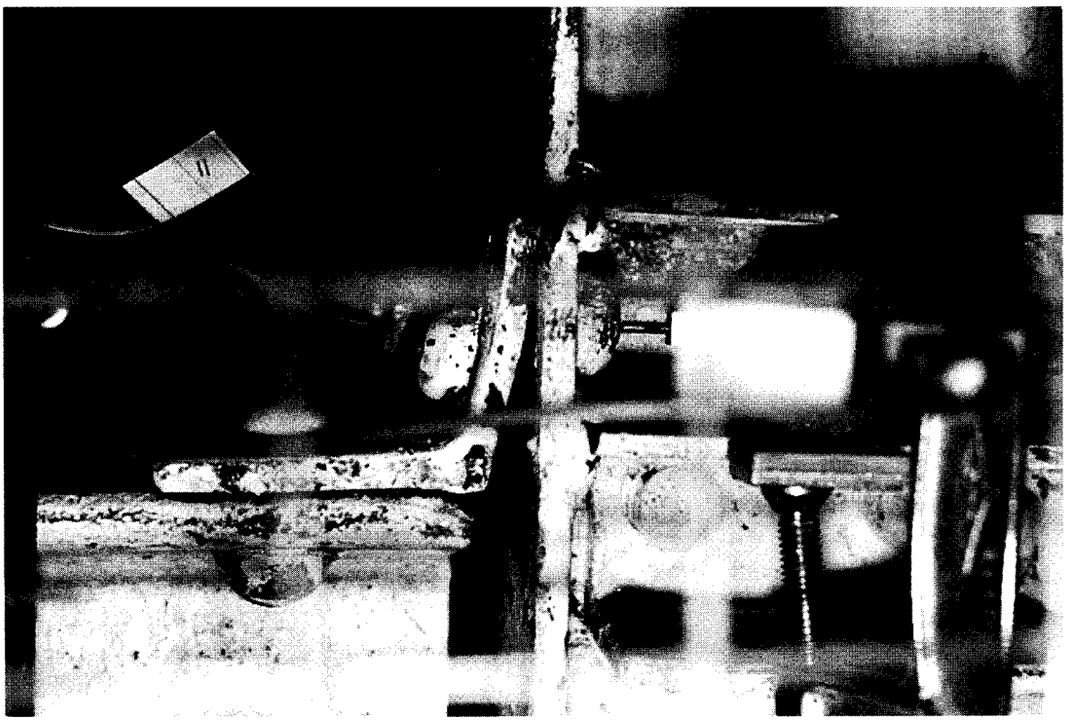

FIG. 4. Top Angle Deformation when Connection is Subjected to Maximum Positive Moment

failed due to bearing failure adjacent to the hole of one of the high-strength bolts in the seat angle.

HYSTERETIC BEHAVIOR OF CONNECTIONS

The M-θ hysteretic curves of the tested connections show a distinct pinching. Since the area under the curves reflects the absorbed energy in each cycle, the presence of highly pinched curves means the energy absorbed by the connection is lower than optimum and reduced by some factors. The main causes of this pinching can be categorized as follows.

Slippage at Rivet Holes

In the very early stages of loading, when the connections are subjected to small shear forces produced by the positive and/or negative moments, pinching can be partly attributed to slippage in the holes of field-driven rivets. This slippage at rivet holes is apparently the result of two contributing factors. One is the lack of tight fit inherent in riveting practices in the past. The standard riveting practice required a minimum hole clearance of 1.6 mm, but specially in the case of field riveting, the center of the rivet holes were not always well matched. In addition, diametric shrinkage after the cooling of hot-driven rivets can also cause small gaps to develop between each rivet's shank and the edge of its hole. The other factor is the insufficient frictional resistance between the connected parts; clamping force due to the pretensioning force of the rivets after cooling is not high enough to prevent slippage by frictional resistance between the connected plates. This is especially true for the rivets driven in the field for which the clamping force appears to be very low, since this operation is accomplished with tools different from those used in shop riveting (Kulak et al. 1987).

Rocking of Top Angles

A typical moment-strain hysteresis, measured at the location of the plastic hinges which developed in the vertical leg of top angles, is shown in Fig. 5 (i.e., by a strain gauge located exactly at middistance from the two rivets of the top angle, and immediately above the angle's fillet). It can be inferred from that curve that the response of the top angles to the reversing force applied to their horizontal leg is also responsible for pinching in the hysteretic curves. When a positive moment is applied to the connection, the resulting and increasing tensile force, which acts on the top angle horizontal leg, eventually causes plastic hinging of the angle and tensile yielding of the rivets. This is the major source of resistance of the top angle. When the load is reversed, instead of a tensile force, a compressive force is applied to the horizontal leg and causes the hinge deformations of the horizontal leg to reverse. However, the plastic hinge mechanism in the vertical leg is not as effective, since the already elongated rivet has lost its ability to provide, by clamping force, a fixed support for the vertical leg of the angle. Moreover, the connection has no natural means of reversing deformation of the already yielded rivet; rivets cannot be compressed by the plates they connect. As a result, without any considerable resistance, the vertical leg rocks over the column flange, i.e., the deformed vertical leg rotates about the hinge in the horizontal leg and the toe of the vertical leg gradually separates from the column face. This continues until the heel of the angle touches the column flange, at which point the compressive load is directly transferred to the column. Therefore, in every cycle, rocking of the angle occurs and causes some pinching in the M-θ curve. A schematic model,

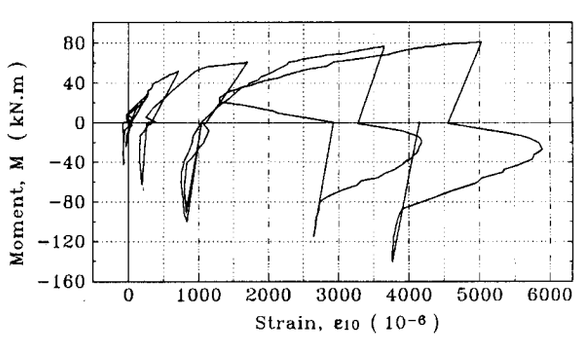

FIG. 5. Moment-Strain Relationship Measured near Location of Plastic Hinge Formed in Vertical Leg of Top Angle

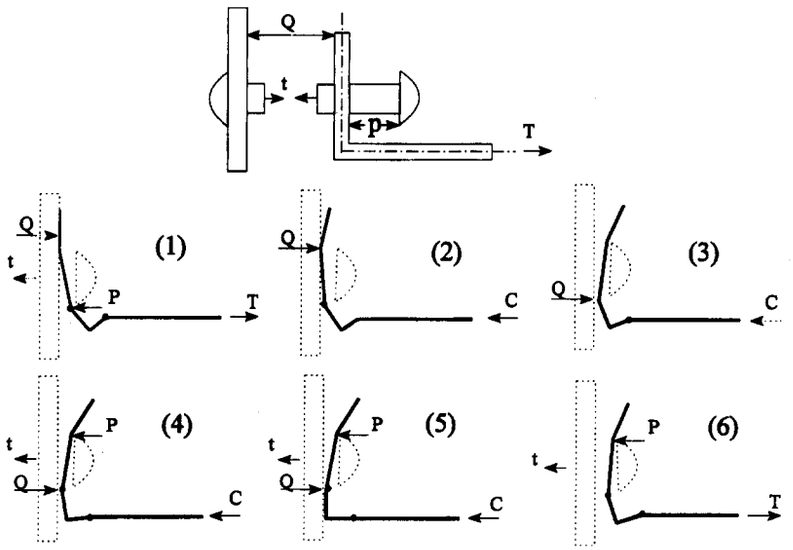

FIG. 6. Different Stages of Top Angle Response to Cyclic Coupling Shear

which illustrates the different stages of response of the top angle, has been developed and is presented in Fig. 6.

This phenomenon also causes a migration of the prying-force reaction point. In design, the prying force is generally assumed to act at the toe of the vertical leg of an angle. However, after a few inelastic cycles, as the vertical legs of the top angles become progressively more convex away from the column, the prying force moves to a point closer to the rivet head, its lever arm becomes shorter, and its value increases to preserve static equilibrium. Consequently, stresses in the rivets are greater than otherwise expected.

Lack of Integrity of Stiffened Seat Connection

Another contribution to pinching is the separation of the seat angle and stiffener angles. Negative moments produce inelastic deformations of both the seat and stiffener angles, i.e., flexural resistance is provided by two separate connection components. However, as the applied moment reverses the yielded stiffeners remain in their position and only the seat angles move back toward the column, gradually separating from the stiffeners. Therefore, stiffeners do not contribute to resisting the horizontal force applied to the seat connection subjected to positive moments, since there are no mechanisms in this connection to force them back under this reversed moment, particularly if the rivets joining the stiffener angles to the columns have yielded in the prior negative moment cycle, as would often be the case. The capacity of the seat connection for loading in that direction is considerably reduced until the seat angles bear anew on the column.

Similarly, in negative flexural excursions, the stiffener angles and the first row of rivets, when already yielded and inelastically deformed, do not provide any resistance until the seat angle deforms sufficiently to touch the stiffener angles, and this can only happen when rotations developed at the connection approximately reach the negative residual rotation obtained in the previous cycle. Therefore, before that value of rotation is reached, no contribution from the stiffener angles is made to the connection resistance.

PHYSICAL MODELS OF EXISTING CONNECTION BEHAVIOR AND CAPACITY

As no physical model for the ultimate limit state of riveted stiffened angle connections existed, and due to the significant dissimilarity in connection behavior under positive and negative moments, two models have been developed to reliably predict these connections' positive and negative moment capacities, respectively.

Positive Moment Capacity

The proposed physical model for the prediction of positive moment capacity, based on the formation of a plastic hinge in the top angle, is conceptually presented in Fig. 7(a). This model assumes a rigid body rotation of the beam about a point located at the tip of the stiffened seat angle. In this model both the top angle and seat angle resistance mechanism contribute to the connection's total moment resistance, M, the former having a dominant effect under positive flexure. For the top angle contribution, the method proposed by Kishi and Chen (1990) for the failure mechanism of top and seat angle connections is not applicable here. That model assumes that two plastic hinges form in the vertical leg of the top angle, one at the edge of the fastener head and the other at the toe of the fillet. However, when the edge of a rivet head is very close to (or overlaps) the toe of the fillet in the vertical leg (as is the case here) only one plastic hinge can develop in the vertical leg and the second plastic hinge required to form a plastic mechanism develops at the toe of the fillet of the horizontal leg of the angle [Fig. 7(b)]. The model proposed here recognizes this behavior.

To obtain the contribution of the top angle connection to moment resistance, the total resisting shear, T, needed to develop the plastic hinge mechanism of the top angle shown in Fig. 7(c) is given by:

$$T = \frac{2m_{p,t}}{h'} = \frac{2\left(\frac{Lt^2}{4}F_y\right)}{h'} = \frac{Lt^2F_y}{2h'} \tag{1}$$

where $m_{p,t}$ = plastic moment capacity of leg of the top angle; h' = vertical distance between the plastic hinges in the top angle (edge of rivets head to midthickness of horizontal leg); and L and t = length and thickness of this angle, respectively.

To find the contribution of the seat angle to moment resistance, the tensile force, T_0, shown in Fig. 7(d), must be evaluated. T_0 is either the minimum tensile yield force of the rivets, T_y, or the value obtained by (2), which is based on failure mechanism of the seat angle shown in Fig. 7(e), and is expressed by

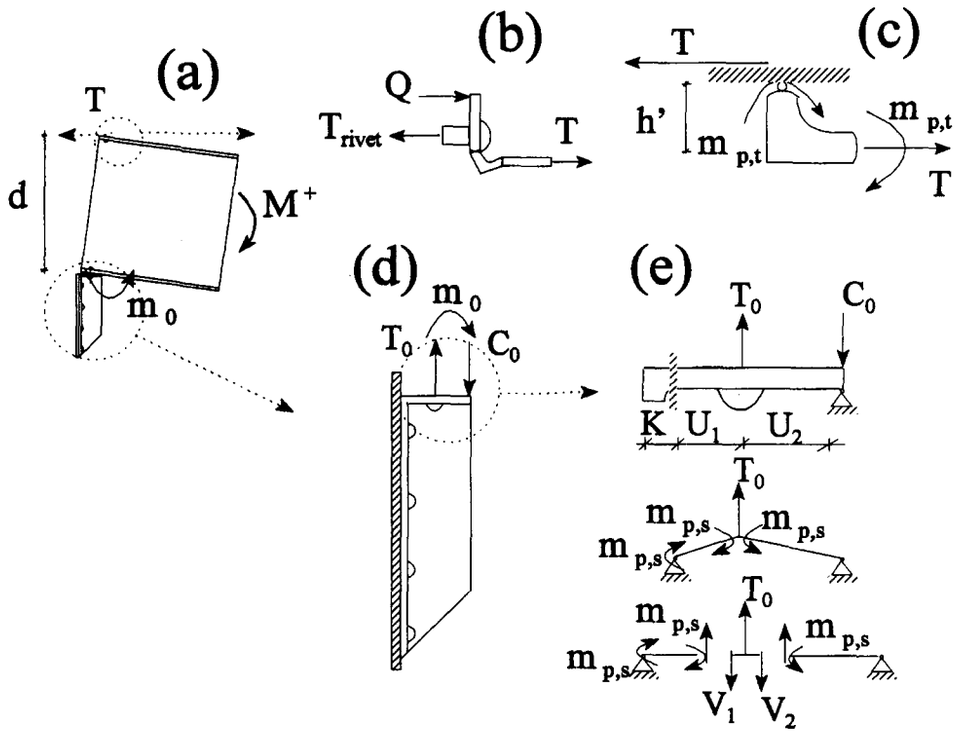

FIG. 7. Plastic Failure Mechanism and Partial Free-Body Diagram of: (a) Full Connection under Positive Moment; (b) Top Angle Connection; (c) Top Angle Fillet; (d) Seat Connection; (e) Seat Angle Horizontal Leg

$$T_0 = V_1 + V_2 \leq \sum_{i=1}^{n} T_{y,i} = 2A_b F_{y,r} \tag{2}$$

where A_b = rivet section area; $F_{y,r}$ = rivet yield stress; and V_1 and V_2 can be determined using the following simple expressions:

$$V_1 = \frac{2m_{p,s}}{U_1}; \quad \text{and } V_2 = \frac{m_{p,s}}{U_2} \tag{3a,b}$$

where $m_{p,s}$ = plastic moment of the seat angle; and U_1 and U_2 = distances shown in Fig. 7(e).

Once T_0 is known, the seat angle resisting moment, m_0, is simply

$$m_0 = T_0 \cdot U_2 \tag{4}$$

Finally, the total positive moment resistance, which includes the contribution from both the top and the seat angle can be determined from the following:

$$M^+ = T \cdot d + m_{p,t} + m_0 \tag{5}$$

in which d = depth of the beam, and all other parameters have been already defined. Numerically, for the connection specimen tested, L = 161 mm, t = 9.5 mm, F_y = 225 MPa, d = 0.507 m, h' = 17.37 mm, U_1 = 31.8 mm, U_2 = 35 mm, A_b = 334.2 mm^2, $F_{y,r}$ = 258 MPa, and a maximum positive moment resistance M^+ of 51 kN·m is obtained. This compares well with the value of 55 kN.m observed experimentally by a change in slope of the M-θ curve. The contribution of the terms $m_{p,t}$ and m_0 in (5) are rather small compared to the term $T \cdot d$.

Negative Moment Capacity

In the absence of an analytical model for the ultimate limit state of riveted stiffened seat angle connections under negative moments, some preliminary analyses were conducted to understand the extent of contribution to the resistance and role of each component of the seat connection in the global failure mechanism. This was done by modeling the stiffener angles as an elastic beam on elastic supports, the stiffness of each support being equal to the longitudinal stiffness of a rivet. This equivalent beam was then subjected to a transverse point load at its end, to represent the shear force applied on the seat angle connection during actual loading of that connection. Results of such analyses showed that the maximum moment in this equivalent beam occurs at the level of the second row of rivets, and that the two rivets in the first row under the seat angle are likely to reach their tensile yield capacity under the magnitude of ultimate loading expected in this case. This led to development of the plastic failure mechanism model of the stiffener angles shown in Fig. 8, which involves formation of a plastic hinge in the stiffener angles and tensile yielding of the first two rivets. Due to compatibility, plastic deformations of the flexible vertical leg of the seat angle must match that of the stiffener angles, which explains the presence of three plastic hinges in this component. This model was also verified by experimental observations.

To find the total failure load using this plastic mechanism, the contribution to shear resistance from the stiffener, F, is first determined by static equilibrium to be

$$F = \frac{m_{p,st} + 2A_b F_{y,r} \cdot l_2}{l_1 + l_2} \tag{6}$$

where $m_{p,st}$ = plastic moment of the stiffener angles; l_1 and l_2 = geometric dimensions shown in Fig. 8; $F_{y,r}$ = yield stress of the rivet steel; and A_b = section area of one rivet. In evaluating F, special care must be taken to correctly locate this force, as the result obtained is very sensitive to the magnitude of the distance, l_1. As substantiated by experimental observations, this distance must be measured from the centerline of the first row of rivets to the end of the stiffener immediately underneath the seat.

An additional force, V, needed to develop the plastic hinge mechanism in the seat angle, also contributes to the total resistance and can be simply determined by

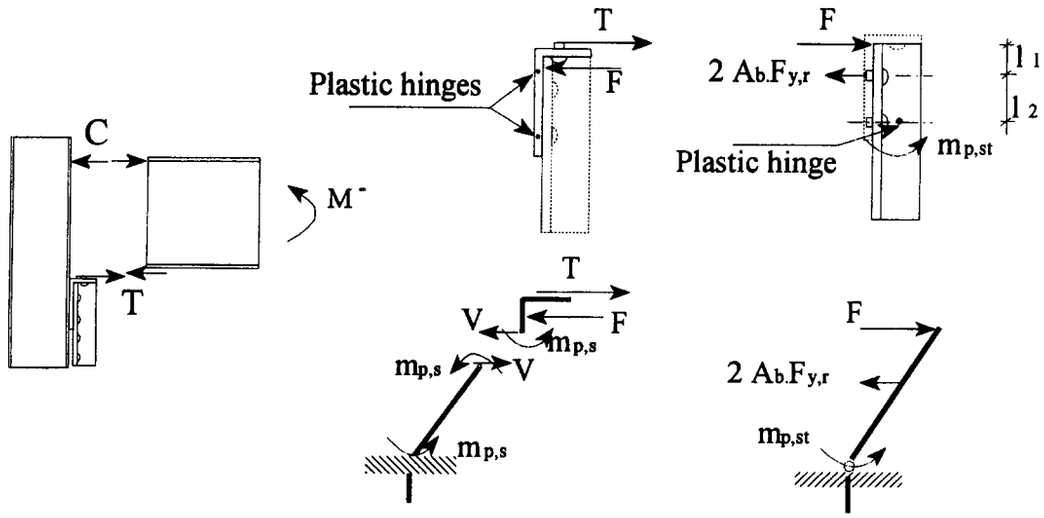

FIG. 8. Ultimate Limit State Model for Prediction of Negative Moment Capacity

$$V = \frac{2m_{p,s}}{l_2} \tag{7}$$

where $m_{p,s}$ = plastic moment capacity of the seat angle; and l_2 is defined in Fig. 8. The total resisting shear, T, then becomes

$$T = F + V \tag{8}$$

and using the depth of the beam h as a lever arm, the resulting total negative moment resistance is

$$M^- = T \cdot d = \left(\frac{m_{p,st} + 2A_b F_{y,r} \cdot l_2}{l_1 + l_2} + \frac{2m_{p,s}}{l_2} \right) \cdot d \tag{9}$$

For the tested existing connections, l_1 = 35.5 mm, l_2 = 75 mm, d = 0.507; $2A_b \times F_{y,r}$ = 172 kN·m; and $m_{p,st}$ = 0.607 kN·m, which give a maximum negative moment resistance, M^-, of 109.7 kN·m. This compares well with the approximate value of 100 kN·m observed experimentally.

RETROFIT STRATEGIES

To this day, retrofitting of existing structures remains more an art than a science. Many retrofit strategies are proposed in the existing literature (FEMA 1992), but these are mostly provided for guidance. The best strategy will vary depending on the circumstances and conditions pertaining to a particular project. A commonly recommended procedure is the addition of new braced or rigid steel frames in an existing building. This approach is well established, effective, and conventional, but can be very costly, particularly since, in many cases, member reinforcements, new foundations, and floor diaphragm reinforcements may be needed to accommodate the new load paths not compatible with the original one, at great disturbance to the occupants if the retrofits are to be accomplished while the building remains in service. Even more difficulties may arise if existing members to be strengthened are not of weldable steel. Moreover, this approach entirely neglects the potential contribution to lateral load resistance of the existing structure, and sometimes overwhelms it when very rigid new structural elements are introduced in the structure. The foregoing conservative solution would also be incompatible with the current intentionally accepted preservation goals for buildings of heritage value which require that retrofitting techniques be as little intrusive as possible, and fully reversible, to allow the future integration of new and less disruptive retrofitting techniques, if ever developed in the future. A solution that can be more harmoniously integrated into the existing fabric of a building would help achieve these goals.

In answer to such concerns, particularly that of making efficient use of the already existing steel structure, alternative retrofitting techniques focusing on the local reinforcing of an individual beam-to-column connection are welcome. Such retrofitting activities can be localized and performed sequentially throughout a building, causing minimum disturbance to occupants. These would also allow seismically induced hysteretic energy dissipation to be uniformly distributed throughout all frame joints.

In that perspective, two different retrofit schemes are proposed to improve the hysteretic behavior of riveted stiffened seat angle connections: (1) The addition of ductile knee braces; and (2) selective welding approach.

Ductile knee braces are easy to design, reliable, inexpensive, and easily replaceable if inelastically deformed. Knee braces can also be easily detailed for the case of nonweldable steel structures. The drawback of this system is its potential intrusiveness at floor levels. However, as heavy nonstructural partition walls in old buildings are often located above the beams, knee braces could be hidden in these walls, those intruding with doorways or other passages simply being omitted.

As for welding, whenever an existing steel structure is of a weldable type of steel, it appears logical to attempt enhancing the cyclic behavior of the connection by welding. Although, converting a semirigid connection into a fully rigid one seems at first to be ideal, this approach may have some shortcomings. The weld preparation is difficult (backup plates, cleanup, etc.), the amount of deposited material is considerable, particularly in the gap almost always present between the column face and end of the beam, the working area is congested, and the weld design can be very complex, in some cases nearly impossible when, for example, columns are made of built-up sections. Moreover, since the columns in old steel buildings were never designed to resist earthquakes and are relatively more flexible than the beams, assuming that the conversion to full fixity was possible, it would create a very dangerous situation by inducing plastic hinges in the column (weak column/strong beam failure mode). Instead, based on a better understanding of the cyclic performance of semirigid connection that resulted from cyclic testing of the existing connection, a more judicious application of welding is possible to greatly enhance the performance of existing connections, eliminating known weaknesses while keeping those inherently good energy dissipating mechanisms already present. In the new proposed "selective weld-

ing'' approach to the retrofit of semirigid connections, weld preparation is limited to the cleaning of surfaces to be welded.

Ductile Knee-Brace Retrofit

The specimen retrofitted using the proposed ductile knee-brace technique is schematically shown in Fig. 9(a). As the number of specimen obtained from an existing building was limited, and because the moment capacity of the original connection in this type of retrofit is not significant considering the relative rigidities of the new and existing components, the specimen previously tested was reused for this retrofit.

In the design of braces, the objective is to maximize the energy dissipation of the knee-bracing system. This desired performance must be achieved within the practical constraints normally encountered when operating on actual buildings. The following design guidelines are proposed:

1. Braces must be long enough to be properly connected to both beams and column (i.e., workability condition). In other words, there should be enough space available for the required welding, gusset plates, etc., at both ends of the brace. On the other hand, if the braces are too long, a larger area of building walls needs to be removed to be able to connect the knee braces to the building steel frame, and/or the braces will be more intrusive. Judgment must be exercised to determine a resonable practical range of brace lengths.
2. Applied moments on beams knee-braced to a column causes tension in one brace and compression in the other. Ideally, the plastic mechanism of the retrofitted connection under the maximum applied moment should develop tension yielding in one brace member and compression yielding in the other, providing a most efficient energy dissipation mechanism. Obviously, it may not be practically possible to achieve perfect axial compression yielding, as the capacity and energy absorption capacity of a member in compression depends on its effective length. Therefore, to maximize capacity and energy absorption of the compressive member, its slenderness ratio should be kept as low as possible. In other words, the C_r/T_r ratio for the member must be as close as possible to 1.0, where C_r and T_r are the compressive resistance and tensile resistance of a member, respectively.
3. To have an efficient, reliable, and easily repairable energy dissipating knee-bracing system, it is desirable to have all plastic hinges form in the compression member itself rather than in the gusset plates or other parts. Thus, braces and gusset plates should be sized to ensure that buckling of the member occurs in the plane of the beam and column. This will also protect walls against out-of-plane induced damage when braces are embedded in walls. The welds to connect knee braces to gusset plate should be designed to provide resistance for development of full tension or compression capacity combined with the plastic moment capacity of the member. Following these design guidelines, an effective length factor, k, of 0.5 can be used in the capacity calculations. Moreover, the braces must be designed to avoid local buckling or torsional buckling prior to formation of the plastic hinges in the compression member.
4. The braces must act as a weak link, i.e., they must yield and dissipate energy. If overly strong braces are used, there would be a risk of forming plastic hinges in the connected columns, which would defeat the intended purposes.

Considering the foregoing requirements and assumptions, the knee braces added to the existing specimen were selected to be standard double angles 25 × 25 × 6.4 mm (1 × 1 × 1/4 in.), designed to develop their ductile plastic mechanism when subjected to a moment of about 190 kN·m, a strength comparable to that of an original stiffened seat angle connection and which also precludes column failure modes. For efficiency and expediency the knee braces were assembled and welded to gusset plates, which were themselves welded to the beams and column instead of being bolted. Bolt holes in bracing members are undesirable as they would reduce the section area of the members in tension, especially for small-size sections similar to those used in this test, and would cause the section to fail at the net area rather than by yielding over the entire member length. Also, for bolted compressive knee

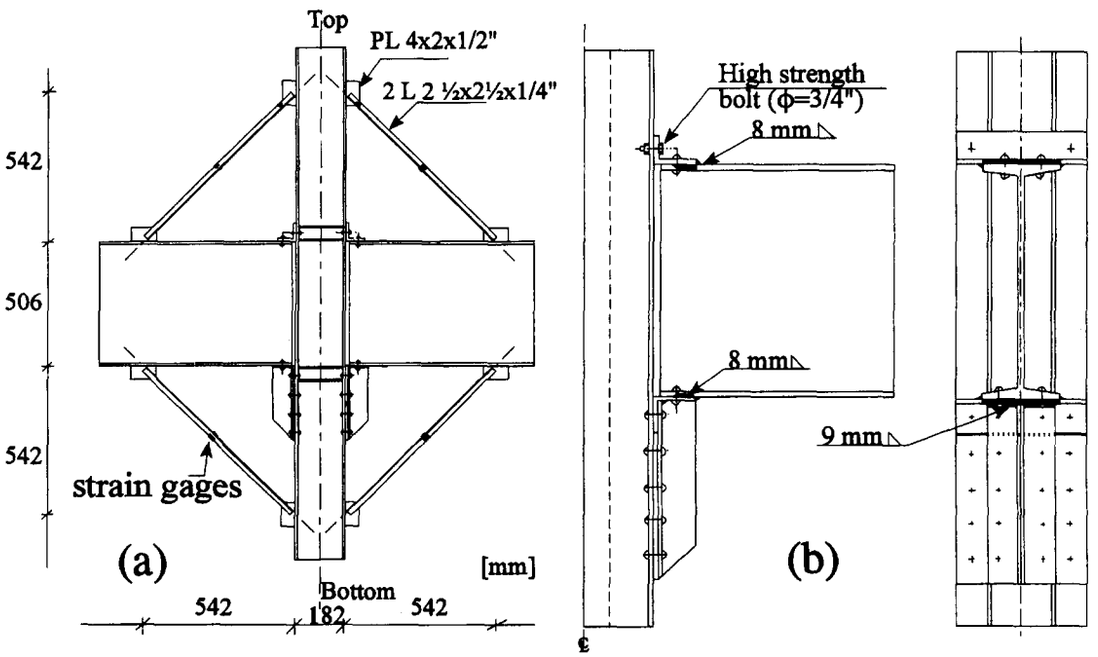

FIG. 9. Retrofit Details: (a) Ductile Knee Braces; (b) Selective Welding

braces, the end plastic hinges could also occur at the net sections having lesser plastic moment capacity. For the same reasons, when existing beams and columns are not of weldable steel, braces should be welded to the web of a T-gusset whose flanges would be bolted to the beam's flanges. Such a connection could be easily designed to comply with the aforementioned performance objectives.

Selective Welding Retrofit

The existing specimen chosen to be retrofitted using the proposed selective welding technique is shown in Fig. 9(b). Its connection detail is somewhat different from that used previously since the column is a built-up shape made of two channels in this case; the steel column was originally enclosed in concrete added for fireproofing purposes, but was exposed at the connection level to be able to perform the proposed retrofit. In spite of the observed differences, the proposed retrofit methodology is still applicable for this connection detail, as the previously described strength mechanisms, and causes for pinching of the hysteretic loops of the stiffened seat angles still exist in this specimen. The retrofit consists of three distinct tasks, as illustrated in Fig. 9(b), and described as follows:

1. Replace selected rivets by high-strength bolts. The extensive yielding and the lack of clamping forces of the four rivets in the top angles have been shown to cause pinching and decrease the moment capacity. Therefore, these are replaced by A490 high-strength bolts of 19 mm (3/4 in.) diameter. None of the other 48 rivets were replaced.
2. Perform selective welding on stiffener angles. To reduce pinching caused by the gap that has been shown to progressively develop between the stiffener angles and seat angles, these two elements are welded together at the location where the gap would be otherwise expected.
3. Perform selective welding on the beam. To increase the connection moment capacity by reducing the risk of the rivet's bearing failure, and to eliminate pinching due to the lack of tight fit and fractional resistance of the rivets connecting the beam flanges to the horizontal leg of the top and seat angles, welding is performed to provide a new load path to transfer shear at that location. Here the weld resistance was designed to be able to resist the full tensile capacity of the angle legs.

EXPERIMENTAL OBSERVATIONS

Ductile Knee-Braced Specimen

The resulting M-θ hysteretic curve for the knee-braced specimen is presented in Fig. 10. It is observed that the hysteretic loops are not pinched in the small range of rotation, but are slightly pinched at larger rotations. Here, positive moments are assumed to cause tension in the top knee braces and compression in the bottom knee braces. Yielding rotation, θ_y, is defined as the point at which brace buckling was first noticed. It occurred at an applied moment of 184 kN·m for a corresponding rotation of 5.1×10^{-3} rad. The specimen in this test reached the maximum moment, M_{max}, of 197 kN·m and developed maximum rotation, θ_{max}, of 29.8×10^{-3} rad, corresponding to a rotation ductility of 5. Brace tension yielding and compression yielding/buckling both effectively contributed to this resistance and energy dissipation; brace tension yielding obviously being the dominant effect. The experiment ended after five cycles, when severe buckling deformations of the knee braces and large rotations were observed, and continuation of the test would likely not have generated any new information. It is noteworthy that a capacity of about 190 kN·m was predicted analytically, neglecting the contribution of the riveted stiffened seat angle connection to the total moment resistance. The knee braces are considerably stiffer and effectively resist nearly all the applied moments.

Selective Welded Specimen

The resulting M-θ hysteretic curve for the selective welding retrofitted specimen, based on the average rotation of connections on both sides of the column, is presented in Fig. 11. A positive yielding rotation of θ_y^+ of 3×10^{-3} rad was obtained when the onset of yielding on the M-θ curve could be first observed, which occurred at a moment of 43 kN·m and negative yielding rotation, θ_y^-, occurred at -6×10^{-3} rad corresponding to a flexural moment of −70.8 kN·m. In the positive yield excursion of the fifth cycle, when the moment reached 60.5 kN·m, developing a rotation of 12.3×10^{-3} rad, fairly large deformations of the angle legs were observed near the heads of the high-strength bolts and adjacent to the fillet of the top angles as a sign of development of a plastic hinge mechanism. By the time the moment reached −116 kN·m, developing a rotation of -22×10^{-3} rad, formation of a plastic hinge mechanism in the stiffener angles, in addition to their limited local buckling, occurred near the level of the second row of the rivets under the seats; the onset of this yielding occurred at about −110 kN·m, detected by strain gauges located on the legs of the stiffener angles at the level of the second row of rivets. Fig. 12 shows the nonuniform inelastic deformations of the vertical leg which typically developed, in this case during the ninth cycle, when the positive moment

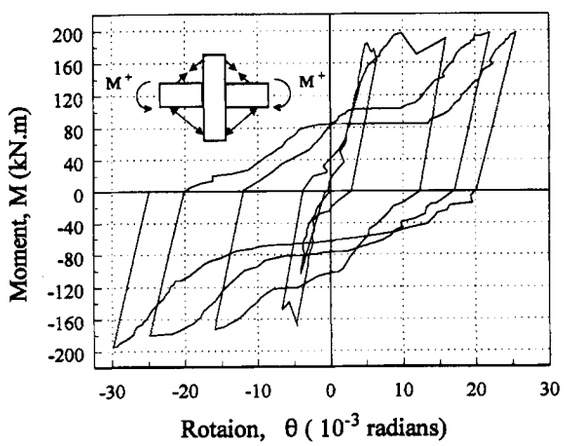

FIG. 10. M-θ Hysteretic Curves Resulting from Testing Knee-Braced Specimen

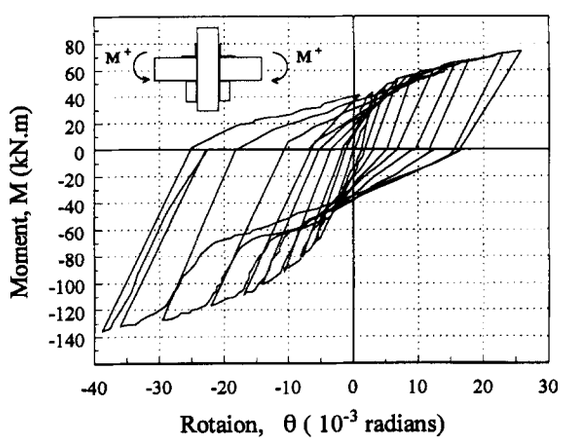

FIG. 11. M-θ Hysteretic Curves Resulting from Testing Selective Welded Specimen

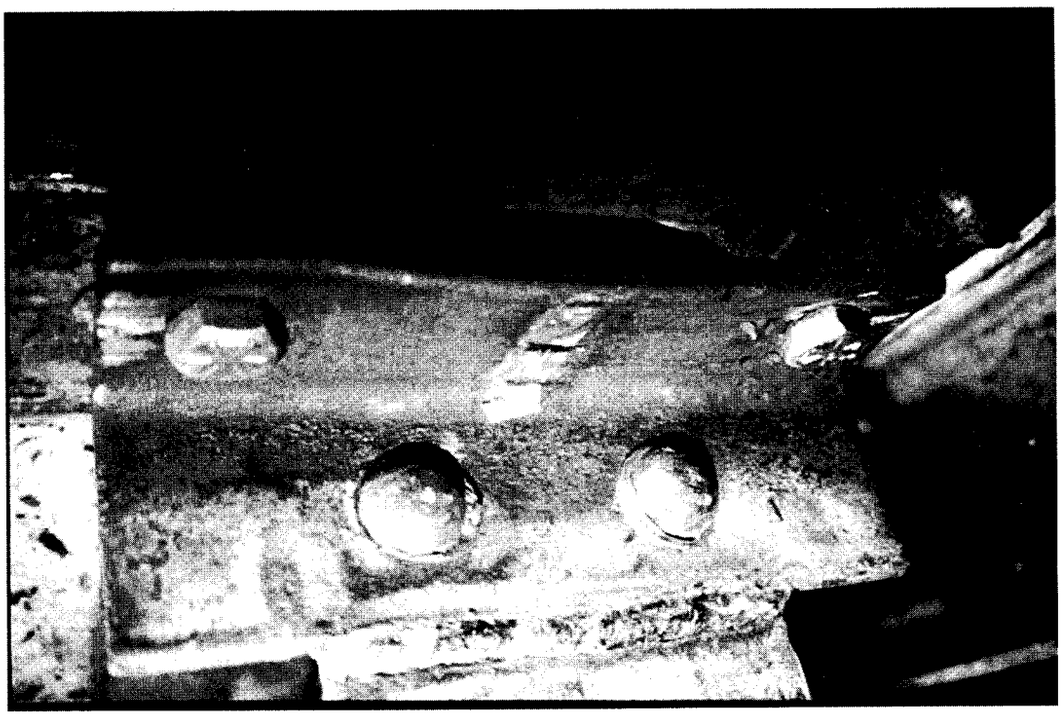

FIG. 12. Nonuniform Inelastic Deformations in Vertical Leg of Top Angle

(a) (b)

FIG. 13. (a) Failure of Seat Angle Connection; (b) Local Buckling of Stiffener Angles

reached 74 kN·m, corresponding to a positive rotation ductility of more than 8.

The specimen was subjected to cyclic loads up to maximum positive, M^+_{max}, of 74 kN·m and maximum negative moment, M^-_{max}, of −136 kN·m. These loads caused maximum positive rotation, θ^+_{max}, of 25.9×10^{-3} rad and negative rotation, θ^-_{max}, of -38.8×10^{-3} rad, respectively. The cyclic part of this experiment ended after 10 cycles when the applied moments caused relatively large inelastic deformations in the seat angles as well as formation of plastic hinges and buckling of the stiffener angles.

Then, for academic interest, it was decided to monotonically subject the specimen to an increasing negative moment until connection failure occurred. As shown in Fig. 13(a), the connection on the left side failed adjacent to the fillet of its seat angle horizontal leg after a rather extreme level of plastic deformations distributed to various parts of the connection. The measured moment corresponding to the failure was −164 kN·m, and maximum negative rotation ductility was about 13 (-77×10^{-3} rad). Local buckling of the stiffener angles was also clearly visible then, as shown in Fig. 13(b) for the unfailed right side connection.

HYSTERETIC RESPONSE OF RETROFITTED CONNECTIONS

Ductile Knee-Braced Connection

The hysteretic loops of the knee braces show a small amount of pinching when large rotations at the joint are developed. This is due to the fact that once a knee brace buckles, its residual deformation and out of straightness cannot be completely eliminated when subjected to tension in the next half-cycle. Moreover, tensile load causes the member to yield and elongate; after each yielding excursion, the stress-free elongated member is longer, and has to buckle just to be able to fit back into the original distance between its supports (gusset plates) connected to fixed points on the beams and the column. Therefore, in every new cycle of this test, buckling occurs sooner than in the previous cycle, because in every new cycle the member is longer than before when unloaded. Consequently, over some range of rotations, all members can be buckled when the specimen is returned to its original position and, then, the capacity of the knee braces is temporarily provided mostly by the compressive members. This is why stocky braces, which can resist loads and dissipate energy while buckling are preferable, even though tension yielding will always eventually develop. While ideally the ratio of C_r/T_r should be chosen as close as possible to 1, it is sometimes practically difficult to achieve this, as in this experiment where the C_r/T_r ratio was 0.8.

Selective Welded Connection

Hysteretic curves for this connection indicate relatively low pinching and, consequently, good energy dissipation. This is mainly due to the several changes made to the connection components, and described earlier in this paper. These components fulfilled their assigned duties effectively and improved the overall behavior of the connection as follows:

1. Absence of visible yielding or cracks in the welds, selectively made to retrofit the connection, showed that these welds can effectively prevent slippage at the holes of the rivets connecting the top and bottom seat angles to the beams under action of the shear forces produced there by the moment at the connection. In addition, these welds increase the specimen's moment capacity by preventing premature bearing failure in these otherwise bearing-type connections.
2. As expected in this experiment, the high-strength bolts provided a sufficiently large clamping force and did not yield, preventing the creation of possible gaps which can cause pinching due to rocking of the vertical legs over the column flanges.
3. As very clearly observed during the test, welding of the stiffener angles to the leg of the seat angles cause these two parts to move together. As such, they both contribute to the flexural resistance, whether the connection is subjected to positive or negative moments.

ANALYTICAL MODEL OF CONNECTION RETROFITTED BY SELECTIVE WELDING

Plastic Mechanism of Wide Top Angle—Positive Moment Capacity

A closer look at the tested connection details revealed that a more complex yield-line pattern developed across the vertical legs and around the location of the high-strength bolts. As a longer top angle was needed to connect the beam to a built-up column section, owing to geometry constraints, the high-strength bolts located in the vertical leg of the top angle are not closely spaced over the length of the angle. That produces nonuniform stresses and deformations in this angle element. Therefore, Kishi and Chen's (1990) assumption that the plastic hinge mechanism of the top angle consists of two straight lines across its vertical leg is not applicable and unconservative in this case. An improved yield-line pattern in the top angle is proposed, and is illustrated in Fig. 14. It is consistent with, and a simplification of experimental observations.

The proposed yield-line pattern for the top angle, and the definition of some geometric parameters are shown in Fig. 14(a). To find the maximum load, P, that can be applied to the top angle, a virtual displacement, Δ, is assumed as shown in Fig. 14(b). On using the principal of virtual work, the upper bound theorem of plastic theory (Horne and Morris 1981), defined in Fig. 4(c), the load P becomes

$$P = t^2 \cdot F_y \left[\frac{h}{(x - b)} + \frac{x}{(h - a)} \right] \tag{10}$$

Where h = height of the angle leg less the size of the angle fillet; a and b = size of the assumed rigid rectangle; t = thickness of the angle leg; F_y = yield stress of the steel; and x = length of the affected region. The unknown, x, which will give the minimum plastic yield capacity, can be obtained by minimizing (10) with respect to x. Doing so gives

$$x = b + \sqrt{h^2 + h \cdot a} \text{ when } x \leq L/2 \tag{11}$$

where L = length of the angle. The capacity of the top angle based on the foregoing model can then be used to predict the positive moment capacity of the connection.

Combining the preceding result with the analytical method presented earlier, the positive moment capacity, M^+, of the riveted stiffened seat angle connection can be predicted for cases where the top angle connection is detailed to join a beam to a built-up column section. For example, for the tested connection that was retrofitted by selective welding, d = 0.506 m, L = 276 mm, h = 59 mm, a = 45 mm, b = 58 mm, t = 8 mm, and F_y = 225 MPa, which gives P = 118 kN. The positive moment yield capacity is simply obtained by multiplying this load, P, by the depth of the beam, d, such that $M^+ = P \cdot d$ = 60.2 kN·m. Results obtained using this assumed rectangular kinematic mechanism are satisfactory, and the additional analytical complexity, which would be introduced by using curved yield lines, is unwarranted.

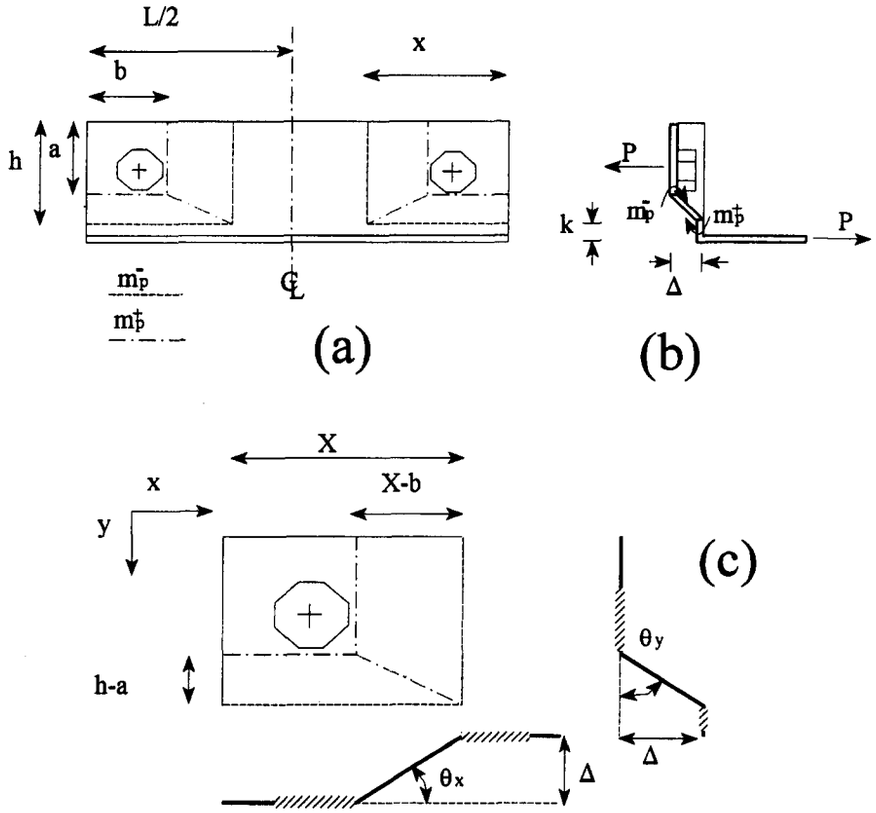

FIG. 14. Plastic Yield Mechanism of Top Angle: (a) Proposed Yield-Line Pattern; (b) Virtual Displacement and External Load *P*; (c) Definition for Angles of Rotations, θ_x and θ_y

Plastic Mechanism of Connection—Negative Moment Capacity

In the absence of knowledge on the ultimate physical behavior of riveted stiffened seat angle connections under negative moments for cases where the connection is detailed to join a beam to a built-up column section, the model proposed here can be reliably used to predict capacity. This model is established by modifying the physical model proposed earlier to account for different connection details and change in behavior of the top and seat angles.

The free-body diagram of the beam end under ultimate negative moment is illustrated in Fig. 15(a). The total resisting shear, T, is again equal to the sum of two forces, F and V shown in Fig. 15(b), which are the contribution of stiffener angles and seat angle to the connection's capacity, respectively.

The seat angle plastic mechanism is shown in Fig. 15(c), and its plastic capacity, V, can be obviously evaluated using (10), i.e.

$$V = t^2 \cdot F_y \left[\frac{h}{(x-b)} + \frac{x}{(h-a)}\right] \leq \sum_{i=1}^{n} T_{yi} = 2A_b F_{y,r},$$

($n = 2$ here) (12)

where T_{yi} = axial yield strength of rivet i; A_b = section area of each rivet joining the seat angle to column flange; and $F_{y,r}$ = rivet yield stress. Contrary to the physical model described earlier, there is no contribution here from the tensile resistance of the first row rivets, which join the stiffener angles to the seat angles. This is because these rivets are not connected to the column flanges in this case and only move as a subassembly of the seat angle and stiffener angle; they never undergo tension. However, those first row rivets that connect the seat angle to the column flange do experience tension, but only limit the maximum load, V, as per (12).

The stiffener angle's contribution to resistance, as illustrated in Fig. 15(d), is given by the horizontal force needed to develop a plastic moment in the stiffener angles at the level of the second row of rivets. Therefore, this resisting force, F, can be expressed as

$$F = \frac{m_{p,st}}{l} \tag{13}$$

where $m_{p,st}$ = plastic moment of the pair of stiffener angles; and l = distance measured from the tip of the stiffener angles to the level of the second row of rivets in the stiffeners as shown in Fig. 15(d).

From the free-body diagram of Fig. 15(a), the total ultimate moment resistance of the connection can be expressed as

$$M = T \cdot d + m_0 \approx T \cdot d = (F + V)d \tag{14}$$

where d = beam depth; and m_0 = moment required to satisfy moment equilibrium on the seat angle element. Due to the uncertainty in formulating a simple free-body diagram, determination of the exact value of m_0 is not easy. However, m_0 obviously cannot exceed the plastic moment capacity of the seat angle leg, $m_{p,s}$, therefore

$$m_0 \leq m_{p,s} = \frac{L \cdot t^2}{4} F_y \tag{15}$$

where L, t, and F_y = length, thickness, and yield stress of the angle. Since, in most practical cases, the value of $m_{p,s}$ is still small compared to the term $T \cdot d$, the value of m_0 can be conservatively ignored when calculating the total negative moment capacity.

Numerically, for the tested specimen that was retrofitted using selective welding, h = 67.5 mm, a = 56 mm, b = 55.8 mm, L = 276 mm, A_b = 334.2 mm^2, $F_{y,r}$ = 258 MPa, l = 114 mm, F_y = 225 MPa, and d = 0.506 m, which gives a negative moment capacity, M^-, of 115 kN·m.

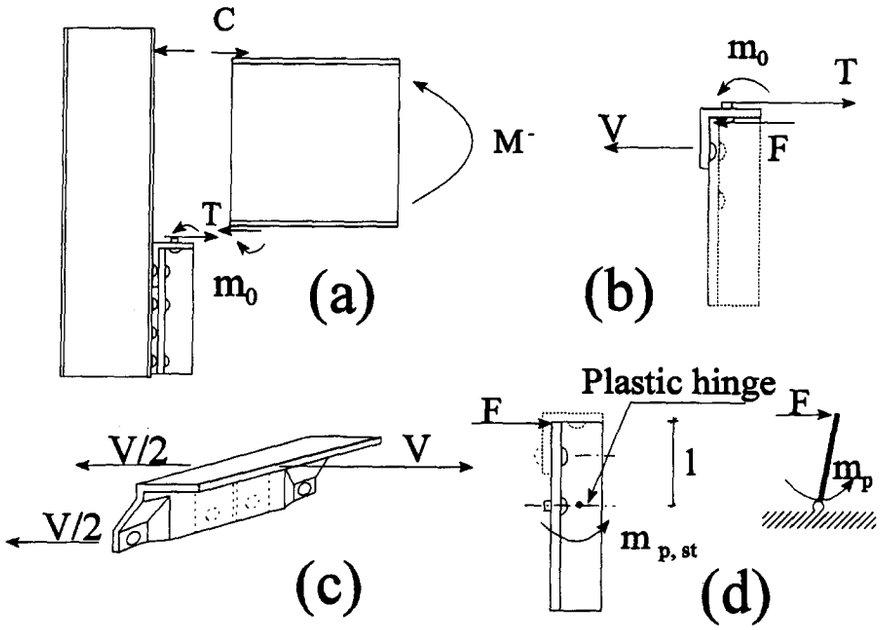

FIG. 15. Analytical Model of Connection at Ultimate: (a) Free-Body Diagram of Beam End under Ultimate Negative Moment; (b) Free-Body Diagram of Seat Angle Assembly; (c) Seat Angle Plastic Mechanism; (d) Free-Body Diagram of Stiffener Angles Assembly

CONCLUSIONS

From this experimental and analytical study of the hysteretic behavior of existing riveted stiffened seat angle connections and two proposed techniques for their seismic retrofit, the following can be concluded.

Although riveted stiffened seat angle connections have not been designed to resist moments, they can develop a considerable moment capacity and exhibit a relatively ductile hysteretic behavior, which could be beneficially considered when evaluating frames built of these connections and subjected to earthquakes.

Although existing riveted stiffened seat angle connections can dissipate energy when subjected to cyclic loads, their hysteretic curves are pinched, even within the elastic range of stress produced in these connections. This pinching can be attributed to different factors, such as slippage in the holes of rivets, rocking of the top angle due to the lack of clamping force and extensive yielding of rivets, and separation of stiffener angles from the seat angle.

The two proposed physical models and the new analytical procedures developed in this study can be effectively used to predict the capacity of the riveted stiffened seat angle connections under both positive and negative moments. The key components of the connections and the mechanism of their contribution to the total moment capacity are identified by this study.

A selective welding retrofit strategy, which consists of performing welds at specific locations of the connection and selectively replacing a few rivets by high-strength bolts, is demonstrated to be an effective retrofit solution which enhances moment capacity and significantly improves the hysteretic energy dissipation capability of riveted stiffened seat angle connections. The selective interventions were carefully chosen to correct previously identified hysteretic weaknesses typical for this type of connection.

Addition of ductile knee braces is demonstrated to be another effective retrofit solution for these steel connections, capable of developing large moment capacities and dissipating considerable energy, in both positive and negative flexure. The design of these special ductile knee braces must, however, follow the guidelines developed in this study to provide conditions leading to efficient energy dissipation in the knee braces, and it should not be erroneously assumed that knee bracing found in existing buildings would provide a satisfactory hysteretic behavior.

The new proposed yield mechanism, which incorporates a modified physical model of the riveted stiffened seat angle connection applicable to angles detailed for built-up columns, can be reliably used to predict plastic moment capacity. For this purpose, new analytical procedures and formulas have been developed. Close correlation with experimental values has been obtained using these models.

Although further investigations are needed to develop hysteretic models that could be used in the nonlinear inelastic seismic analysis of steel frames having retrofitted connections, the proposed retrofitting schemes and ultimate plastic models presented in this study provide practicing engineers with valuable insight into the hysteretic behavior and potential resistance of these existing and retrofitted connections, particularly when the seismic resistance of old steel frames built with such connections is a concern. Moreover, since the tests were conducted on full-scale specimens taken from an existing building, the proposed and tested retrofit schemes are demonstrated to be practical solutions which could be readily implemented. The retrofitting schemes proposed in this paper are believed to be advantageous as they can be conducted locally, with minimum intervention to the existing frames and minimum disturbance to the occupants or the fabric of heritage buildings. However, while awaiting the results of nonlinear inelastic analysis of full structures, engineers are cautioned to use judgment and pay particular attention to drift and P-Δ issues when using these retrofit solutions.

ACKNOWLEDGMENTS

The writers are grateful for the cooperation of Peter McCourt of National Capital Commission, John Cooke, of John Cooke & Associates Ltd., and Paul Greenspoon, of Greenspoon Bros. Ltd, for their cooperation in obtaining the test specimen from the demolished Daly building in Ottawa. This research program was partly funded by the Natural Science and Engineering Research Council of Canada. This support is sincerely appreciated. However, the opinions expressed in this paper are those of the writers and do not reflect the views of the aforementioned sponsor or individuals.

APPENDIX I. REFERENCES

Astaneh, A., Nader, M. N., and Malik, L. (1989). "Cyclic behavior of double angle connections." *J. Struct. Engrg.*, ASCE, 115(5), 1101–1118.

Federal Emergency Management Agency (FEMA). (1992). "NEHRP handbook for seismic rehabilitation of existing buildings." *Rep. FEMA-172*, Washington, D.C.

Horne, M. R., and Morris, L. J. (1981). *Plastic design of low-rise frames*, Granada Publication, London, England, 15–16.

Jones, S. W., Kirby, P. A., and Nethercot, D. A. (1982). "Columns with semirigid joints." *J. Struct. Engrg.*, ASCE, 108(2), 361–372.

Kishi, N., and Chen, W. F. (1990). "Moment-rotation relations of semirigid connections with angles." *J. Struct. Engrg.*, ASCE, 116(7), 1813–1834.

Kulak, G. L., Fisher, J. W., Struik, J. H. A. (1987). *Guide to design criteria for bolted and riveted joints*, 2nd Ed., John Wiley & Sons, Inc., New York, N.Y.

Leon, R., Forcier, G. P., Roeder, C. W., and Preece, F. R. (1994). "Cyclic performance of riveted connections." *Proc., 12th ASCE Struct., Congr.*, ASCE, New York, N.Y., Vol. 2, 1490–1495.

Lewitt, C. W., Chesson, E., and Munse, W. H. (1966). "Restraint characteristics of flexible riveted and bolted beam-to-column connections." *Rep.*, Dept. Civ. Engrg., Univ. of Illinois, Urbana, Ill.

Marly, M. J., and Gerstle, K. H. (1982). "Analysis and test of flexibly-connected steel frames." *Rep. Prepared for AISC under Proj. 199*, Am. Inst. of Steel Constr. (AISC), Chicago, Ill.

Maxwell, S. M. et al. (1981). "A realistic approach to the performance and application of semi-rigid joints in steel structures." *Joints in structural steel work*, J. H. Howlett, W. M. Jenkins, and R. Stansby, eds., Pentech Press, London, England, 2.71–2.98.

Moore, H. F., and Wilson, W. M. (1917). "Tests to determine the rigidity of riveted joints of steel structures." *Engrg. Experiment Station, Bull. No. 104*, Univ. of Illinois, Urbana, Ill.

Nader, M. N., and Astaneh, A. (1989). "Experimental studies of a single story steel structure with fixed, semi-rigid and flexible connections." *Rep. No. UCB/EERC-89/15*, Earthquake Engrg. Res. Ctr., Univ. of California, Berkeley, Calif.

Radziminski, J. B., and Azizinamini, A. (1986). "Low cyclic fatigue of semi-rigid steel beam-to-column connections." *Proc., 3rd U.S. Nat. Conf. on Earthquake Engrg.*, Earthquake Engrg. Res. Inst. (EERI), El Centro, Calif., Vol. 2, 1285–1296.

Rathbun, J. C. (1935). "Elastic properties of riveted connections." *Trans. ASCE*, ASCE, New York, N.Y., Paper No. 1933, Vol. 11, 524–563.

Sarraf, M. H. K. M. (1993). "Experimental study on cyclic behavior of riveted stiffened seat angle connections," MS thesis, Ottawa-Carleton Inst. for Civ. Engrg., Univ. of Ottawa, Ottawa, Ont., Canada.

Stefano, M., Luca, A., and Astaneh, A. (1994). "Modeling of cyclic moment-rotation response of double-angle connections." *J. Struct. Engrg.*, ASCE, 120(1), 212–229.

Young, C. R., and Jackson, K. B. (1934). "The relative rigidity of welded and riveted connections." *Can. J. Res.*, Vol. 11, 62–100.

APPENDIX II. NOTATION

The following symbols are used in this paper:

A_b = section area of rivet shank;
a, b = vertical and horizontal length of fastener clamping zone;
d = beam depth;
F = stiffener angle's contribution to resistance;
F_y = yield stress of steel section;
$F_{y,r}$ = yield stress of rivet steel;
h = width of affected plastic zone;
h' = distance between location of plastic hinges in top angle;
k = size of angle fillet;
L = total length of angle;
l = longitudinal distance measured from tip of stiffener angles to second row of rivets;
l_1, l_2 = distance between centerline of rivet in stiffener angles;
M = total resisting moment of connection;
M^+, M^- = positive and negative moment resistance of connection;
m_p = plastic moment of angle leg;
m_p^+, m_p^- = positive and negative plastic moment per unit length of angle leg;
$m_{p,s}$ = plastic moment of seat angle leg;
$m_{p,st}$ = plastic moment of pair of stiffener angles;
$m_{p,t}$ = plastic moment of top angle leg;
m_0 = seat angle moment resistance;
P = load resistance corresponding to plastic mechanism of angle;
T = total shear resistance;
T_{yi} = yield strength of rivet;
T_0 = seat angle tensile resistance;
t = thickness of angle leg;
U_1, U_2 = spacing of rivets in seat angle connection;
V = seat angle's contribution to resistance;
V_1, V_2 = vertical shear components in seat angle;
x = length of affected plastic zone;
Δ = virtual displacement;
θ = connection rotation; and
θ_x, θ_y = rotation of plastic zone of angle with respect to the x and y axis.